

Link-up of 90° domain boundaries with interface dislocations in BaTiO₃/LaAlO₃

Z. R. Dai^{a)}

Beijing Laboratory of Electron Microscopy, Chinese Academy of Sciences, P.O. Box 2724, Beijing 100080, and Department of Materials Physics, University of Science and Technology-Beijing, Beijing 100083, People's Republic of China

Z. L. Wang^{b)}

School of Materials Science and Engineering, Georgia Institute of Technology Atlanta, Georgia 30332-0245

X. F. Duan

Beijing Laboratory of Electron Microscopy, Chinese Academy of Sciences, P.O. Box 2724, Beijing 100080, People's Republic of China

Jiming Zhang^{c)}

Advanced Technology Materials, Inc., 7 Commerce Drive, Danbury, Connecticut 06810

(Received 11 January 1996; accepted for publication 20 March 1996)

Interface microstructures of BaTiO₃/LaAlO₃ grown by metalorganic chemical vapor deposition (MOCVD) are studied using high-resolution transmission electron microscopy (HRTEM). Interface dislocations in BaTiO₃/LaAlO₃ have been shown to be directly linked up with the 90° domain boundaries in BaTiO₃. This association is a result of strain relief due to a phase transformation when cooled down from the growth temperature. The Burgers vector of the interface dislocations is $\langle 010 \rangle$.

© 1996 American Institute of Physics. [S0003-6951(96)00422-6]

Epitaxial growth of barium titanate (BaTiO₃) thin film has attracted much attention because of its potential application in microelectronics and integrated photonics.¹ The film-substrate interfacial structure plays an important role in determining the quality of the film. Misfit dislocations are usually produced at the interface to partially relieve the strain due to lattice mismatch.^{2,3} BaTiO₃ experiences a phase transition from a cubic to a tetragonal phase during cooling, resulting in the formation of 90° and 180° domain boundaries. It is important to understand the formation mechanism of domain boundaries and its dependence on the microstructure of the film-substrate interface, because the physical properties and performance of this ferroelectric film are largely determined by the domain structures. In this letter, the interface structure between BaTiO₃ and LaAlO₃ is examined to show the association of 90° domain boundaries at interface dislocations. The mechanism that drives this link-up is discussed.

Epitaxial BaTiO₃ thin film was deposited on LaAlO₃ (001) by metalorganic chemical vapor deposition (MOCVD) as reported elsewhere.⁴ Cross-sectional samples were prepared to examine the interfacial structure at 200 kV using a JEOL 2010 high-resolution transmission electron microscope (HRTEM).

BaTiO₃ has a cubic perovskite-type structure ($a=0.4012$ nm) above 120 °C.⁵ Below 120 °C, it is tetragonal ($a=0.3992$ nm, $c=0.4036$ nm).⁶ The tetragonal BaTiO₃ phase has ferroelectric property because of the spontaneous polarization along the c axis. A 90° domain boundary is formed if the c axis in one domain is parallel to the ab axis

of another domain. At room temperature, LaAlO₃ has a perovskite-like structure with a slight rhombohedral distortion ($a=0.3788$ nm, $\alpha=90^\circ 4$ ft.).⁷ LaAlO₃ experiences a phase transition from a rhombohedral to a cubic structure ($a=0.381$ nm) at 435 °C.

Figure 1(a) shows a low-magnification TEM image of a

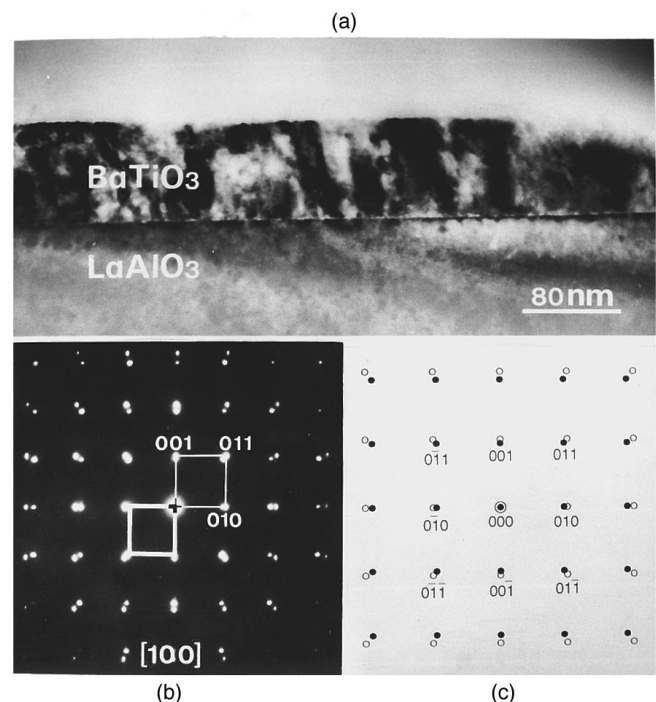


FIG. 1. (a) A TEM image of a cross-sectional sample of BaTiO₃/LaAlO₃ (001). The film growth direction is [001]. (b) A [100] electron diffraction pattern of the film showing epitaxial growth of the film. (c) A calculated pattern corresponding to (b), in which open circles denote the Bragg reflections from LaAlO₃ and solid circles from BaTiO₃. All the indexes are marked according to LaAlO₃ crystal.

^{a)}Electronic mail: khkuo@image.blem.ac.cn

^{b)}Corresponding author: Electronic mail: zhong.wang@mse.gatech.edu

^{c)}Current address: Motorola Inc., 3501 Ed Bluestein Blvd., Austin, TX 78721.

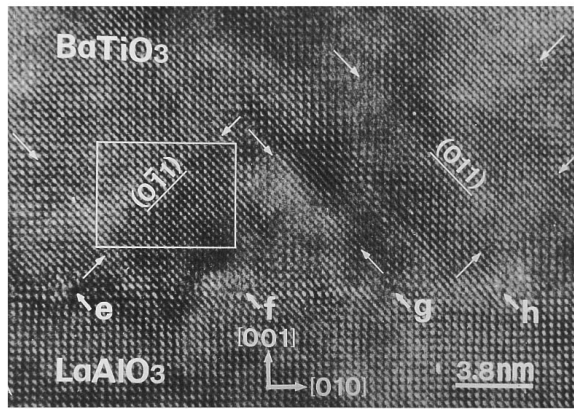


FIG. 2. A [100] cross-sectional HRTEM image of BaTiO₃/LaAlO₃. Thick white arrowheads indicate the positions of interface dislocations. Thin white arrowheads indicate the 90° domain boundaries in BaTiO₃.

cross-section sample. An electron diffraction pattern from this specimen [Fig. 1(b)] shows the epitaxial growth of the film. Two sets of diffraction spots are seen in Fig. 1(b), one belonging to BaTiO₃ (thick white line square) and the other belonging to LaAlO₃ (thin white line square). The lattice mismatch between BaTiO₃ and LaAlO₃ produces the splitting of the diffraction spots. Since the distortion of LaAlO₃ from cubic structure is extremely small, the relative rotation between BaTiO₃ and LaAlO₃ is hardly detected by electron diffraction. Therefore, the orientation relationships between the film and the substrate almost exactly satisfy (001)_{BTO}|| (001)_{LAO}, (010)_{BTO}|| (010)_{LAO}. At room temperature, BaTiO₃ has a tetragonal structure with $c/a=1.01$. The small difference between a and c axes is hardly resolved in the electron diffraction pattern, thus, the indexes of the diffraction patterns are labeled according to a cubic structure. A calculated electron diffraction pattern by assuming the above epitaxial relation is shown in Fig. 1(c), in good agreement with Fig. 1(b).

Figure 2 shows a cross-section HRTEM image of the interfacial region. Interface dislocations are seen, as indicated by thick white arrowheads. The distance between dislocations f and g is 7.3 nm, which is close to the theoretically expected value 7.2 nm, while the distance between dislocations e and f (8.3 nm) is larger than the calculated value and the distance between dislocations g and h (5.4 nm) is smaller than the expected value. These data indicate that the interface strain is distributed inhomogeneously. 90° domain boundaries are observed in the image (thin white arrowheads). The domains boundaries are parallel to (011) and (01̄1) and form a 45° angle with the interface, and these boundaries are the 90° a - a type.^{8,9} An enlargement of the region included in the white line square in Fig. 2 is shown in Fig. 3. The domain boundary is indicated by a thick white line. The relative rotation of the crystal across the domain boundary can be seen along the thin white lines. This is a typical character of the 90° a - a domain boundary.

A remarkable phenomenon seen in Fig. 2 is that the 90° domain boundaries in BaTiO₃ are directly associated with the cores of interface dislocations. Interface dislocations are generated to relieve the strain produced by lattice mismatch. When the film undergoes a structure transformation from a

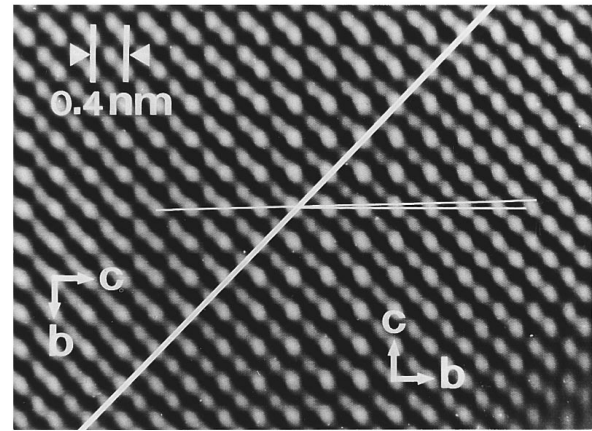


FIG. 3. An enlarged, Fourier filtered image of a region enclosed by a white line square in Fig. 2. The thick white line indicates a 90° domain boundary and the thin white line shows a relative tilt of lattice planes on both sides of the boundary.

cubic to a tetragonal phase during cooling from the growth temperature, strain is also produced in the film due to both the lattice mismatch and difference in thermal expansion coefficients between the film and the substrate, domain boundaries are formation to accommodate the strain.¹⁰ The lattice mismatch is 5.3% at the growth temperature (800 °C). At room temperature, as the result of cubic to tetragonal phase transformation, the lattice mismatch is still 5.3% if the c axis of the film is perpendicular to the interface, but the lattice mismatch is 6.5% if the a axis of the film is perpendicular to the substrate. Therefore, the lattice mismatch experiences a jump at the domain boundary, resulting in accumulated strain at the boundary region. Also, the different lattice mismatches

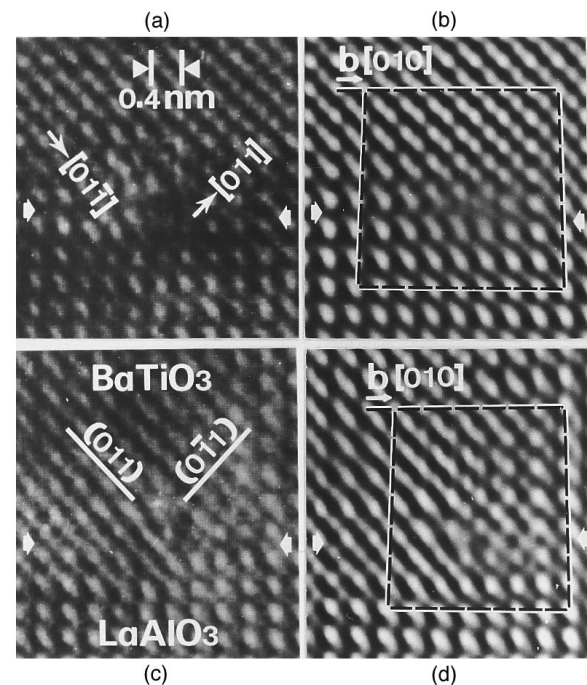


FIG. 4. Enlarged images of the regions around the dislocation e (a) and the dislocation h (c) in Fig. 2. (b) and (d) are the Fourier filtered images corresponding to (a) and (c), respectively. White arrowheads indicate the interface between BaTiO₃ and LaAlO₃. The Burgers circuits around the dislocation cores are indicated.

in the two adjacent domains will result in different intervals of interface dislocations, as observed in Fig. 2.

Domain boundaries are formed at the transformation temperature (120 °C), and they may move freely at this temperature and tend to move towards the sites that have lower energy. When a domain boundary is directly linked to an interface dislocation, the strain fields of the two might partially cancel out, resulting in lower energy. Thus, the domain boundary is likely to be “pinned” at the dislocation site. Although the domain formation in thin ferroelectric films is a rather complex phenomenon, it is generally believed that the size and density of the boundaries are largely determined by the constraints at the interface. Since the density of interface dislocation is determined by the lattice mismatch, a proper choice of substrate lattice mismatch and symmetry of the surface of the substrate and the thermal mismatch as well could have a significant effect on the density and size of domain boundaries formed in ferroelectric thin films. This may have an important impact on the performance of the films.

Figures 4(a) and 4(c) show enlarged images around the regions of dislocations *e* and *h* in Fig. 2, respectively, and the processed images [Figs. 4(b) and 4(d)]. By drawing the

enclosure circuits for Burgers vectors, as indicated in Figs. 4(b) and 4(d), the Burgers vector of the interface dislocations is determined as [010] (equivalent to [100] or [001]), an edge type.

In conclusion, interface dislocations in BaTiO₃/LaAlO₃ have been shown to be directly linked up with the 90° domain boundaries in BaTiO₃. The interface dislocations in BaTiO₃/LaAlO₃ are the <100> edge type.

¹W. Ousi-Benommar, S. S. Xue, R. A. Lessard, A. Singh, Z. L. Wu, and P. K. Kuo, *J. Mater. Res.* **9**, 970 (1994).

²J. Chen, L. A. Wills, and B. W. Wessels, *J. Electron. Mater.* **22**, 701 (1993).

³V. P. Dravid, H. Zhang, L. A. Wills, and B. W. Wessels, *J. Mater. Res.* **9**, 426 (1994).

⁴J. Zhang, G. J. Cui, D. Gordon, P. Van Buskirk, and J. Steinbeck, *Mater. Res. Soc. Symp. Proc.* **310**, 249 (1993); J. Zhang, R. A. Gardiner, P. S. Kirilin, R. W. Boerstler, and J. Steinbeck, *Appl. Phys. Lett.* **61**, 2884 (1992).

⁵H. D. Megaw, *Proc. R. Soc. A* **189**, 261 (1947).

⁶R. G. Rhodes, *Acta Crystallogr.* **4**, 105 (1951).

⁷S. Geller and V. B. Bala, *Acta Crystallogr.* **9**, 1019 (1956).

⁸M. Tanaka and G. Honjo, *J. Phys. Soc. Jpn.* **19**, 954 (1964).

⁹Y. H. Hu, E. M. Chan, X. W. Zhang, and M. R. Harmer, *J. Am. Ceram. Soc.* **69**, 594 (1986).

¹⁰R. Bruinsma and A. Zangwill, *J. Phys. (Paris)* **47**, 2055 (1986).